

Paper:

A New Ultrasonographic Image Displaying System to Support Vein Detection

Shuhei Noyori*, Gojiro Nakagami*, Hiroshi Noguchi**, Koichi Yabunaka*,
Taketoshi Mori**, and Hiromi Sanada*

*Departments of Gerontological Nursing/Wound Care Management, Graduate School of Medicine, The University of Tokyo
7-3-1 Hongo, Bunkyo-ku, Tokyo 113-0033, Japan

E-mail: {noyori-ty, gojiro-ty, kyabunaka-ty, hsanada-ty}@umin.ac.jp

**Department of Life Support Technology (Molten), Graduate School of Medicine, The University of Tokyo
7-3-1 Hongo, Bunkyo-ku, Tokyo 113-0033, Japan

E-mail: {hnogu-ty, tmoriics-ty}@umin.ac.jp

[Received September 21, 2016; accepted December 26, 2016]

The insertion of a peripheral intravenous catheter is often required by patients during a hospital stay. However, approximately 30% of intravenous catheters experience catheter failure. Using ultrasonography to observe the depth and diameter of a vein and to thereby perform catheter site selection is a promising procedure to prevent catheter failure. Nevertheless, it is difficult to perform this procedure, as it is associated with complicated maneuvering in which a nurse simultaneously manipulates an ultrasonographic probe, assesses veins, and inserts a catheter. In this study, a new image displaying system that consists of a camera, head-mounted display, and software is proposed. The newly developed image-processing program detects the fingertip of a user, and the system displays the reconstructed ultrasonographic image at any cross-sectional plane as indicated by the user's finger. Additionally, veins are superimposed on the ultrasonographic image, and the depth and diameter of veins are also displayed on the image. The newly developed image-processing algorithm detects markers and fingertip in the images captured by the head-mounted camera by robustly detecting the fingertip. This aids in realizing a new ultrasonographic image displaying system. This system is used to increase the success rate of vein detection by nurses in a study of volunteers.

Keywords: nursing assessment support, vascular access, ultrasonography, head-mounted display

1. Introduction

Almost 70% of patients require peripheral intravenous catheter (PIVC) insertion during hospital stays for treatment and monitoring [1]. However, nearly 30% of intravenous catheters involve some form of failure [2], and this is known as catheter failure (CF). Measures for eliminating CF are required as CF causes unnecessary catheter

replacement or medical procedures and reduces quality of life for patients.

Multiple puncture attempts are associated with CF in PIVC, and it was suggested that these attempts could cause inappropriate selection of vessels for catheter insertion [3]. Therefore, it is important to select the best area of an available blood vessel to reduce the number of puncture attempts. There is also a possibility that PIVCs could be inserted into different veins as they are repeatedly inserted in both inpatients and ambulant patients for treatments and examinations. Therefore, it is necessary to detect the appropriate veins available to aid in preventing CF related to PIVC. However, the selection of an appropriate vein requires extensive experience and skill [4] and is a difficult task for nurses with less clinical experience. These nurses mainly select veins for PIVC based on the visibility of veins and do not place much weightage on other factors including vein diameter and the path of the vein and nerves. Selecting appropriate veins to prevent CF requires a precise assessment of vein diameter and depth. This can be achieved through the development of vein visualization devices.

Devices using near-infrared (NIR) light were developed to aid visualization and identification of vessels by projecting an image of the vessels on the skin surface. However, in clinical studies, the usage of NIR devices did not improve the success rate for puncture [5–7]. Therefore, the applicability of these devices was not assessed because the two-dimensional image of the veins offered by these systems lacked information related to vein depth [6] and could even overestimate the diameter of superficial veins [6, 7], which could lead to an attempted cannulation of veins that would be appropriately rejected without the device [7]. Thus, it is necessary for devices that help nurses in detecting veins to precisely display three-dimensional structures including vein diameter and depth.

Ultrasonography (US) is a promising candidate that supports site selection via three-dimensional observation of veins. Specifically, US is a non-invasive and precise modality that can visualize subcutaneous structures in



cross-sectional images. Recent studies revealed the characteristics of veins appropriate for PIVC insertion with US (e.g., vein depth and diameter) [8–10], and thus US is a promising candidate to also assist nurses with PIVC site selection.

The present study explores a new system to assist nurses in the selection of PIVC insertion sites by using US. There are two methods for US site selection, namely real-time imaging and prelocation. In real-time imaging, which is also referred to as the US-guided technique, a nurse can observe the vein and the surrounding structure and simultaneously insert the PIVC. This technique is recommended for central venous catheterization (CVC) with respect to an internal jugular vein [11]. A robot assisting real-time US-guided central venous catheterization was developed [12]. However, with respect to PIVC insertion, the real-time technique requires extensive training because the peripheral veins are narrower than the central vein, and thus can be easily occluded by probe pressure. Additionally, repeated examination for appropriate veins by US at each PIVC insertion is difficult in clinical settings given that catheters are replaced several times during hospitalization. Conversely, with respect to prelocation, US images are previously obtained in which a nurse marks the skin over a candidate vein as a line or dots with a felt-tipped pen using US. Subsequently, the nurse inserts a catheter along the marking without a US. Therefore, it is not necessary for the nurse to manipulate the US probe during the insertion procedure. Therefore, prelocation is a better method for PIVC insertion.

The utilization of prelocation methods is subject to two major problems. First, it is difficult to memorize the three-dimensional structure obtained by the previous scan. That is, the usage of pre-scanned US images requires a nurse to memorize information acquired from the US image of the PIVC insertion candidate area for accurate vein selection. The simplest way to avoid this problem involves placing a mark on the patient's skin to indicate the appropriate vein. However, other information, such as vein depth and diameter, are also required. Therefore, a system displaying pre-scanned US images, which correspond to the referred site at each assessment timing, is a solution to detect veins by performing an inspection with three-dimensional information. The other problem is related to image display. It is necessary for a nurse to shift their gaze between the display and the patient when a nurse observes US images shown in a display located away from the site for insertion (e.g., US monitor display on the equipment). Thus, it is extremely likely that turning away from the insertion site will interrupt the procedure. A head-mounted display (HMD) could be a practical solution for the nurse to observe the US image without moving his/her eyes. Extant research has examined the usability of HMD for US image display with respect to CVC [13] and PIVC [14] insertion.

In order to offer a clinically applicable system, it is necessary to resolve the problem of integrating the two major methods for PIVC insertion site selection, namely palpation and US image display by prelocation. In clinical set-

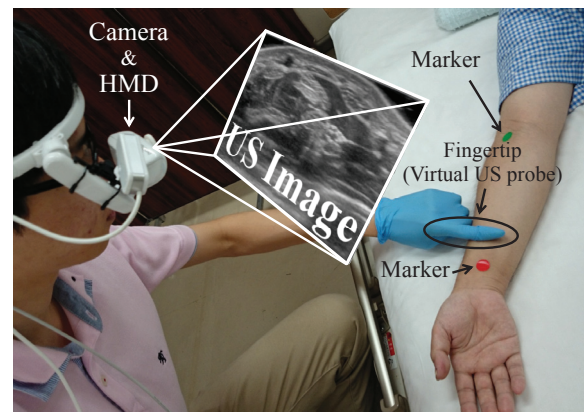


Fig. 1. Concept of the virtual ultrasonic probe system.

tings, palpation is important for the evaluation of veins [4] and should not be hindered. Additionally, it is also necessary for the US image operation to be simple and easy because it is highly likely that a nurse may not possess experience related to the operation of US devices. In order to solve this problem, the current study presents a “virtual ultrasonic probe” in which a nurse’s finger is used as an image-selecting tool similar to an ultrasonic probe. This new system can be used by a nurse to select a US image from the pre-scanned stock of US images by pointing a fingertip on the patient’s arm. This technique does not interrupt vein palpation and simultaneously provides a nurse with information regarding the veins including vein depth and diameter. Therefore, a nurse can easily detect appropriate veins for PIVC insertion.

The aim of this study involves the construction of a virtual ultrasonic probe system to support appropriate vein and site selection for PIVC. This system enables a nurse to observe US images without hindering inspection, palpation, or other procedures and to select appropriate veins for PIVC insertion. The effectiveness of this system was examined with respect to supporting vein detection by nurses in a study of volunteers.

2. Virtual Ultrasonic Probe System

In this study, a new virtual US probe system was developed to help nurses in selecting an appropriate vein by displaying the vein and surrounding structure with pre-scanned US images (**Fig. 1**). This system consisted of hardware including a camera and an HMD that obtained movies and displayed US images, and software that enabled the user’s finger to virtually act as a US probe.

The system is used by nurses as follows. A nurse scans the patient’s forearm with a US probe when a patient is admitted to a hospital or when a PIVC is inserted for the first time during hospitalization. Three-dimensional US data is then calculated based on the captured US images. Nurses use a virtual US probe system when they select a vein and a site for PIVC. A nurse points his or her finger on the patient’s forearm with the HMD and camera on

the head, and the image processing software then detects the finger from the captured image and calculates the relative position and direction of the finger to the patient's forearm. The virtual two-dimensional US image at the specific point is then generated and displayed with vessel information. In order to achieve the same operability, the displayed US images are two-dimensional and the information related to vein depth and diameter is superimposed on the US image. A nurse can observe subcutaneous tissues, assess veins based on the information related to vein depth and diameter, and then determine the site at which the PIVC should be inserted.

2.1. System to Reconstruct and Display US Images

2.1.1. In-Advance US Image Acquisition

The anterior surface of the forearm was used in this study to simplify the US image acquisition procedure. Position markers were attached on the wrist and cubital fossa of the anterior surface of the forearm. This was followed by capturing US images from the wrist marker position to the cubital fossa marker position at a uniform speed by using a linear-array probe (included in Noblus, Hitachi Aloka Medical, Ltd.), which is suitable to observe superficial structures with a tourniquet placed on the patient's arm. A linear-array transducer (5–18 MHz) was used under measuring conditions that were identical to those used in a previous study [3]. The focal range and the image depth to determine the correct display range when US imaging was performed corresponded to 1.5–2.5 cm. The echo gain and the dynamic range were tuned to a proper level to observe the veins.

2.1.2. Display of the US Images

It was assumed that a patient's arm was scanned at a uniform speed, and thus the position of the user's fingertip was associated with the probe location at pre-scanning. The fingertip was detected in each frame captured by a camera mounted near the user's eyes based on the color of the glove that is typically worn by nurses. The attached markers were detected to estimate the positions of the wrist and the cubital fossa in each frame. The relative position and direction of the user's finger to the patient's forearm was then calculated. Finally, the US image of the site as indicated by the fingertip was generated from the three-dimensional data and displayed on the HMD with vessels and the information superimposed on the US image.

2.2. Hardware

A see-through HMD (AiRScouter WD-200S, Brother Industries, Ltd) was adopted. Images could be displayed on this HMD with a high resolution, which enabled nurses to select the site for PIVC by observing the US images. A camera (UCAM-C0220FEWH, ELECOM Co., Ltd.) was attached on the HMD. The camera image was used to detect position markers and the user's finger. The field of

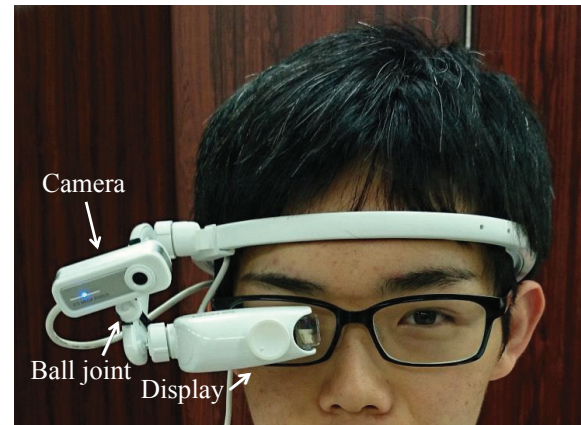


Fig. 2. Hardware. A see-through HMD is adopted, and images are displayed on this HMD at a high resolution. A camera is attached on the HMD using a ball joint, which allows the user to adjust the field of view of the camera such that it covers the entire forearm area.

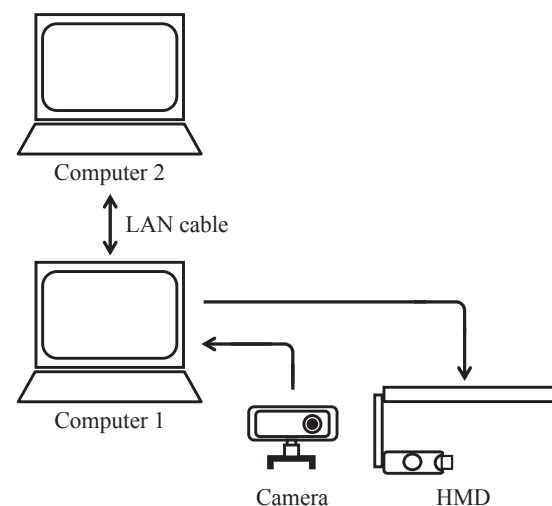


Fig. 3. System configurations. The virtual ultrasonic probe system is operated on computer 1 (C1). Computer 2 (C2) is used for the US image storage and reconstruction of the virtual cross-sectional image. Each frame captured by the camera is sent to C1. The C1 then computes the position and the direction of the finger by the fingertip detection program and sends the parameters to C2. A virtual cross-sectional US image is reconstructed based on the parameters. The image is then sent to HMD via C1. Finally, the image is displayed on the HMD.

view (FOV) of the camera was sufficiently large to visualize the entire forearm area. A ball joint was used to attach the camera, which allowed users to adjust the FOV of the camera to cover the entire forearm area (Fig. 2).

2.3. Software

The software consisted of a marker and finger detection part (Section 2.3.1) and a US image display part (Section 2.3.2). Two computers (C1 and C2) were used for each calculation as shown in Fig. 3. Specifically, C1 was

used for the marker and finger detection part, and C2 was used for the US image storage and reconstruction of the virtual cross-sectional image.

2.3.1. Fingertip Detection

An image-processing program to detect the position markers and the fingertip was developed using OpenCV.¹ Two circular position markers (red and green stickers) were used to estimate the position of the wrist and the cubital fossa. The red marker was placed on the wrist, and the green marker was placed on the cubital fossa.

Robust and real-time detection of the markers and user's finger is crucial in realizing the virtual ultrasonic probe. The combination of shape and color information is useful for robust detection. The features of the curvature of the contour of the fingertip and the parallel lines of finger side edges provided important clues to estimate the fingertip position. With respect to real-time detection, the position history calculated in the previously captured image was used to reduce the computational cost, and this enabled the detection of the location even in cases when the markers were missed.

Additionally, it is necessary for the parameters representing position and direction of the fingertip to be stable to reconstruct virtual cross-sectional US images. The lack of stability reduced the usability of identifying US images based on the fingertip position. The actual direction of a finger rarely changed during palpation or movement of the position of the finger, and thus the use of the estimated fingertip position history could resolve the estimation instability. This could be achieved by a filtering technique. A Kalman filter was introduced as a filtering technique to implement this idea. The parameters of covariance for both the process and observation noise were empirically tuned.

The following section provides an explanation of the marker detection algorithm by using the red marker as an example. Each input image was converted into a HSV color space that was robust to changes in the lighting condition. The red area was defined as $h < 10$ or $170 < h$ and $150 < s$ (HSV of OpenCV is defined as $0 < h < 180$, $0 < s, v < 255$). The areas with the fore-mentioned conditions were extracted. A search for a marker was initiated in the 60×60 pixel square around the previous marker position when the red marker was detected in the previous frame. With respect to the i -th area, the geometric center ($\mathbf{r} = (r_x, r_y)$) and the diameter of the smallest enclosing circle (c_i) were computed. The displacement vector (d_{marker}) from the previous marker to \mathbf{r} and the ratio of the parameters, $r_{\mathcal{A}_i} = |d_{\text{marker}}|/c_i$, were then calculated. With respect to the areas with $r_{\mathcal{A}_i} < 0.75$, the size (a_i) of the area and the edge length of the smallest enclosing rectangle (long side l_i and short side s_i) were computed. This was followed by calculating the ratios of the parameters, $r_{\mathcal{M}_i} = c_i/l_i$, $r_{\mathcal{m}_i} = s_i/l_i$. The area with the appropriate conditions ($0.9 < r_{\mathcal{M}_i} < 1.1$, $0.9 < r_{\mathcal{m}_i}$ and $200 < a_i$) was estimated as the red marker. The marker

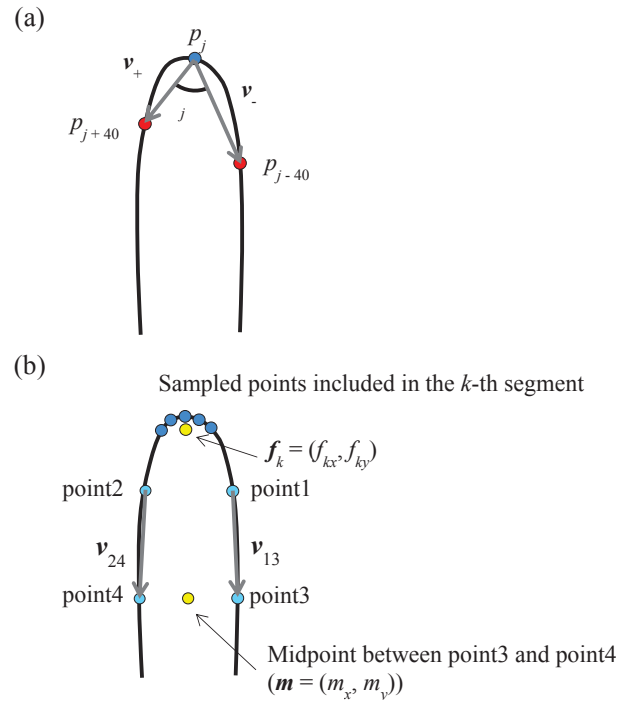


Fig. 4. Fingertip detection algorithm. (a) The curvature of the contour around each sampled point is evaluated. When the curvature is large, the point is estimated as located around a fingertip. (b) When v_{13} and v_{24} are parallel, the k -th segment is estimated as a fingertip. The fingertip position is defined as the average point of the sampled contour points. The direction of the finger is defined as $\mathbf{v}_{\text{direction}} = \mathbf{f} - \mathbf{m}$.

was searched for again as follows when the marker was not detected. Each area with $r_{\mathcal{A}_i} < 0.5$ was examined if it satisfied $0.5 < r_{\mathcal{M}_i} < 1.5$, $0.5 < r_{\mathcal{m}_i}$, and $100 < a_i$. The detecting algorithm allowed the robust detection of the markers while accommodating for temporary changes in brightness and viewpoint. The green area was defined as $50 < h < 80$ and $s > 70$ and was detected with the same algorithm. The position of the green maker was defined as $\mathbf{g} = (g_x, g_y)$.

When both markers were detected, the position and the direction of the fingertip were estimated with an algorithm similar to that used in a previous study [15]. Four steps were involved in estimating the position and the direction.

First, the hand wearing a blue glove was detected as the largest blue area. The blue areas were defined as $90 < h < 110$, $s > 150$, and $v > 80$.

Second, a fingertip was extracted from the hand area based on shape characteristics. Contour points were extracted from the hand area. The extracted points were down-sampled into one of seven points ($p_j; j = 0, \dots, N$) to reduce the curvature computation cost. The vectors from p_j to the point p_{j-40} and p_{j+40} (v_- and v_+) were computed, and the angle ($0^\circ < \theta_j < 180^\circ$) and the cross product ($cp_j = v_+ \times v_-$) between the vectors were calculated (Fig. 4). The determination of more than four adjacent contour points with the condition $\theta_j < 60^\circ$ and $0 < cp_j$ implied that the contour around the points cor-

1. Itseez, "OpenCV," <http://opencv.org/> [Accessed September 1, 2016]

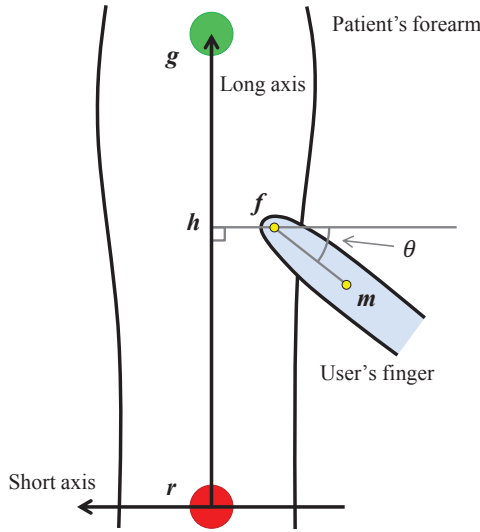


Fig. 5. Process to calculate the relative finger position and direction. The relative position and direction of the finger are represented by the following three parameters: the ratio of the long axis (r_{lax}), the ratio of the short axis (r_{sax}), and the angle (θ) that is defined as $r_{lax} = |\mathbf{v}_{lax}|/|\mathbf{v}_{rg}|$ ($0\% \leq r_{lax} \leq 100\%$), $r_{sax} = |\mathbf{v}_{sax}|/|\mathbf{v}_{rg}|$ ($-30\% \leq r_{sax} \leq 30\%$), and θ , which corresponds to the angle between vector FM and vector IF ($-180^\circ \leq \theta \leq 180^\circ$).

responded to a strong peak, and the points were treated as a single segment (a fingertip contour candidate). With respect to the k -th segment, the geometric center $\mathbf{f}_k = (f_{kx}, f_{ky})$ among points that indicates the fingertip position and the displacement ($\mathbf{d}_{fingertip}$) from the previous fingertip position were computed. Contour points near the k -th segment were assessed to examine as to whether the fingertip position candidate \mathbf{f}_k corresponded to the actual fingertip position. If \mathbf{f}_k corresponded to the actual fingertip position, then the contour points at both sides of the k -th segment would form two parallel lines. Cosine ($\cos \theta_k$) of the angle between two vectors (\mathbf{v}_{13} and \mathbf{v}_{24}) that consisted of four points (point1–point4) were calculated (Fig. 4). The points were obtained from the contour points at a distance along the contour from both sides of the k -th segment. The distance was empirically determined based on the finger length in the captured images. When the conditions $|\mathbf{d}_{fingertip}| < 40$ (\mathbf{f}_k was located near the previous fingertip position) and $\cos \theta_k < 0.9$ (\mathbf{v}_{13} and \mathbf{v}_{24} were parallel) were satisfied, the \mathbf{f}_k was estimated as the actual fingertip position $\mathbf{f} = (f_x, f_y)$.

Third, the direction of the fingertip was computed. The midpoint $\mathbf{m} = (m_x, m_y)$ between point 3 and point 4 was determined, and the direction of the fingertip was defined as $\mathbf{v}_{direction} = \mathbf{f} - \mathbf{m}$.

Finally, the relative position and direction of the fingertip to the markers were calculated (Fig. 5). They were represented by the following three parameters: the ratio for the long axis (r_{lax} [%]), the ratio for the short axis (r_{sax} [%]), and the angle (θ [°]). The intersection ($\mathbf{h} = (h_x, h_y)$) of a line segment between two markers and the perpendicular line from \mathbf{f} to the segment was

computed. This was followed by defining $\mathbf{v}_{rg} = \mathbf{g} - \mathbf{r}$, $\mathbf{v}_{lax} = \mathbf{h} - \mathbf{r}$, and $\mathbf{v}_{sax} = \mathbf{f} - \mathbf{h}$. The three parameters are then defined as follows:

$$r_{lax} = \frac{|\mathbf{v}_{lax}|}{|\mathbf{v}_{rg}|} \quad (0\% \leq r_{lax} \leq 100\%), \quad \dots \quad (1)$$

$$r_{sax} = \frac{|\mathbf{v}_{sax}|}{|\mathbf{v}_{rg}|} \quad (-30\% \leq r_{sax} \leq 30\%), \quad \dots \quad (2)$$

where a negative value of r_{sax} indicates that the fingertip is located lateral to the markers.

When r_{sax} is less than -30% or more than 30% , the fingertip was estimated as outside of patient's forearm area and was determined as lost. The parameter θ is defined as the angle between $\mathbf{v}_{direction}$ and \mathbf{v}_{sax} . With respect to each parameter, noise was filtered using a Kalman filter adopting a random walk model [16]. The estimation (\mathbf{x}_t) and the observation (\mathbf{y}_t) of the true state at frame t are defined as follows:

$$\mathbf{x}_t = \begin{bmatrix} \hat{r}_{lax} \\ \hat{r}_{sax} \\ \hat{\theta} \end{bmatrix}, \quad \dots \quad (3)$$

and

$$\mathbf{y}_t = \begin{bmatrix} r_{lax} \\ r_{sax} \\ \theta \end{bmatrix}. \quad \dots \quad (4)$$

The Kalman filter assumed that \mathbf{x}_t evolved from the state \mathbf{x}_{t-1} at frame $(t-1)$ based on the following equation where \mathbf{v}_{t-1} denotes the process noise, which is assumed to be drawn from a multivariate normal distribution with covariance \mathbf{Q} as follows:

$$\mathbf{x}_t = \mathbf{F}\mathbf{x}_{t-1} + \mathbf{v}_{t-1}, \quad \dots \quad (5)$$

where

$$\mathbf{F} = \begin{bmatrix} 1 & 0 & 0 \\ 0 & 1 & 0 \\ 0 & 0 & 1 \end{bmatrix},$$

$$\mathbf{v}_{t-1} \sim N(0, \mathbf{Q}), \quad \mathbf{Q} = \begin{bmatrix} 0.2 & 0 & 0 \\ 0 & 0.2 & 0 \\ 0 & 0 & 0.2 \end{bmatrix}.$$

At frame t , the observation (\mathbf{y}_t) of the true state was estimated based on the following equation where \mathbf{w}_t denotes the observation noise, which is assumed to be drawn from a multivariate normal distribution with covariance \mathbf{R} as follows:

$$\mathbf{y}_t = \mathbf{H}\mathbf{x}_t + \mathbf{w}_t, \quad \dots \quad (6)$$

where

$$\mathbf{H} = \begin{bmatrix} 1 & 0 & 0 \\ 0 & 1 & 0 \\ 0 & 0 & 1 \end{bmatrix},$$

$$\mathbf{w}_{t-1} \sim N(0, \mathbf{R}), \quad \mathbf{R} = \begin{bmatrix} 2 & 0 & 0 \\ 0 & 2 & 0 \\ 0 & 0 & 9 \end{bmatrix}.$$

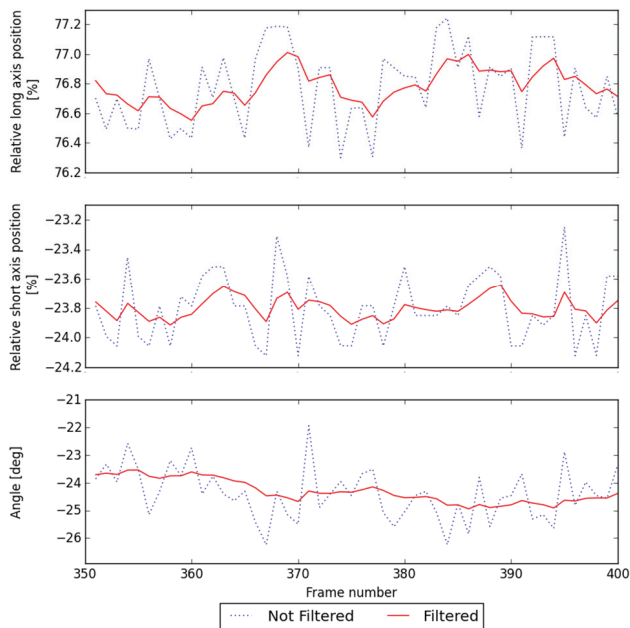


Fig. 6. Denoising by Kalman filtering. With respect to each parameter, the noise is filtered by a Kalman filter by adopting a random walk model. The filtered values are stable when compared with non-filtered values.

The parameters \mathbf{Q} and \mathbf{R} were empirically determined. A typical example of the filtered result is shown in **Fig. 6** when a finger moves smoothly on the arm. The graph indicated that values of the parameters were stabilized.

The distance between the two position markers approximately corresponded to 200 mm and 200–300 pixels in the captured images. Therefore, the distance resolution of the finger position estimation approximately corresponded to 1 mm. Specifically, because the position was estimated by the relative position between the markers (0%–100%), the minimum step approximately corresponded to 2 mm (= 200 mm/100%).

The estimated parameters \mathbf{x}_t were transmitted to the US image displaying software. The result of the marker and finger detection is shown in **Fig. 7(a)**.

2.3.2. US Image Display Corresponding to Fingertip Position and Direction

The display software could display the cross-sectional US image (virtual US image) at any position and direction using the voxel image based on pre-scanned two-dimensional short-axis US images.

A virtual US image was created based on pre-generated voxel data with the vessel information. The three-dimensional map that contains all the brightness of US data as a voxel was calculated using pre-scanned two-dimensional short-axis US image sequence. It was assumed that the US probe moved horizontally on the arm surface in a uniform speed without rotation. Based on this assumption, the voxel width and height were determined by the resolution of US image. The width and height corresponded to 38.0 mm / 682 pixel and 21.0 mm /

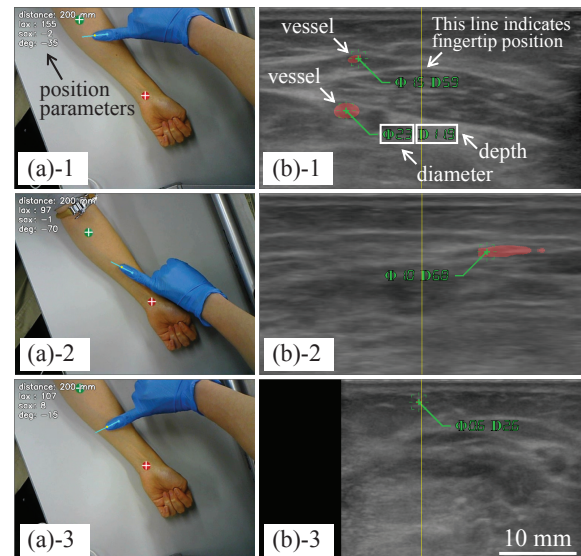


Fig. 7. Examples of the processing results and reconstructed US images corresponding to the fingertip position. (a) Detected markers are indicated by a white cross. The fingertip is indicated by a point and a line that represented the center and the width, respectively, of the virtual ultrasonic probe. (b) The US image is reconstructed from the short-axis US images, and colored vessels are superimposed on the image. The depth and diameter of the vessels are also indicated. The vein is located just under the fingertip when the vertical line overlaps with the vein in the US image.

380 pixel, respectively. The resolution of depth was determined based on the distance between two markers and the number of captured image frames. A usual pre-scanning determined the distance as approximately 200 mm, and the number of frames approximately corresponded to 200. However, nine artificial images were inserted between two captured US images as the resolution considerably exceeded the width and the height. The artificial images were generated by interpolating the US image brightness in linear per pixel. The depth resolution was ten times larger, and it was similar to the width and the height. The increased resolution provided a smooth image while generating virtual US images in the rotated probe location.

In order to display vessel information with the virtual US image, the vessel information was also prepared from the captured US images. The vessel areas in each image frame were manually drawn with a red color as the US images were too unstable and cluttered to automatically detect vessel areas. The development of an automatic detection algorithm from US images is beyond the scope of the present study and will be examined in a future study. Based on the drawn images, the other three-dimensional map that contains vessel areas was generated to color the vessel area in the virtual US image. Centers, diameters, and distances between the center of vessels and the forearm surface of each drawn area in each frame were also calculated from the drawn images to display vessel information including diameter and distance from the surface.

The virtual US images were generated from the pre-

pared data. The transition matrix was calculated based on the location and rotation on the arm surface as measured by a head-mounted camera. The three-dimensional location of each pixel in the virtual US probe was calculated using this matrix. The brightness in the map with three-dimensional pixel location corresponded to the brightness of pixel in the virtual probe. Similarly, the vessel three-dimensional map was detected as to whether or not the pixel was inside the vessel. The transparent red color was drawn over the virtual US brightness color if the pixel was located in the vessel. Vessel information, such as diameter, was detected by searching an intersection point of the virtual probe plane with respect to segments of blood vessel centers. The vessel information of the intersected point was displayed near the points in the virtual US image. The vertical line was also illustrated in the virtual US image to aid the easy perception of a finger point on an arm. Typical examples of the generated virtual US images are shown in **Fig. 7(b)**.

3. Experiments and Results

An experiment was conducted to evaluate whether the system performed as expected. The experiment protocols are discussed in the following section.

First, the veins were assessed by a nurse with several years of clinical experience and proficiency in PIVC insertion. The nurse's assessment was accompanied by the recruitment of an adult woman whose veins could not be easily detected as a simulated patient. The nurse attached small circular stickers to the veins on the anterior surface of the participant's left forearm detected by the nurse's inspection and palpation with a tourniquet. This was followed by attaching position markers for image processing, and an expert sonographer scanned the anterior surface from the wrist marker position to the cubital fossa marker position at a uniform speed using a linear-array probe.

Nurses were recruited as test users. Participating nurses were asked to detect the maximum possible number of veins on the anterior surface of the patient-role participant's left forearm by using a tourniquet. The participating nurses first searched for veins by inspection and palpation. The nurses then searched again with the system. In both trials, the detected veins were marked by attaching small circular stickers, and the locations were recorded by capturing photographs. The tasks were performed in this order to prevent a carry-over effect caused by memorizing information from US image that could affect vein detection without the system.

The result was evaluated by examining as to whether three specific veins, namely the median antebrachial, basilic, and cephalic veins (**Fig. 8**), into which the PIVC is often inserted were detected. The number of detections was compared between trials with and without the system. A researcher determined as to which vein was detected based on the sticker sites and the veins in the US image. A vein was determined as detected when a sticker

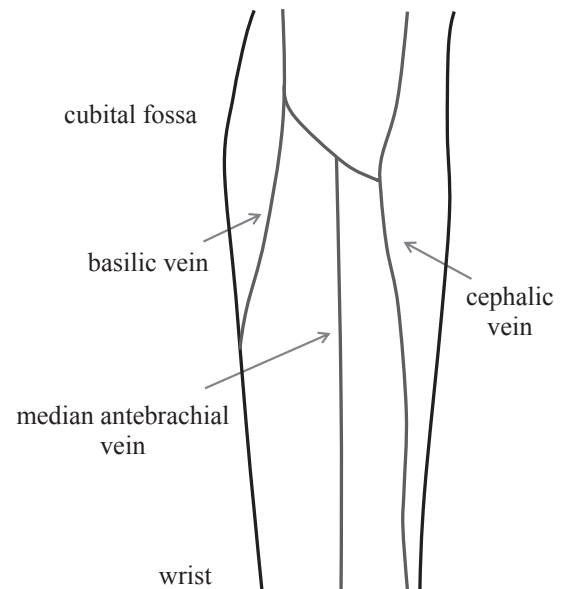


Fig. 8. Cutaneous veins on the anterior surface of the left forearm.

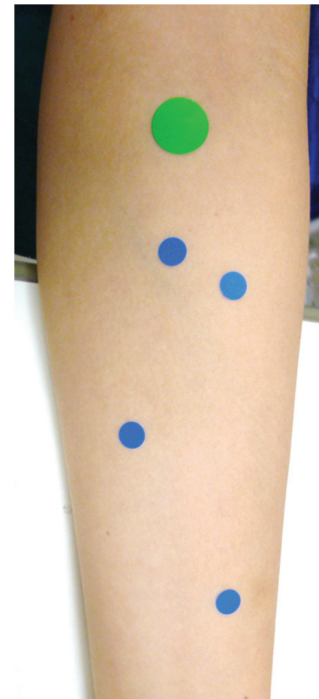


Fig. 9. Veins detected in the experiment. Circular stickers are attached on the veins detected by an expert nurse.

was attached on it at any point in the anterior surface of the forearm (**Fig. 9**).

All participants were adequately informed of the experiment and expressed their freely given informed consent under consideration of ethical issues. The participants were also informed of the right to refuse to participate in this experiment or to quit participating at any point of time without any repercussions.

Five registered nurses participated in this experiment.

Table 1. Number of participants who could detect each vein ($N = 5$). The number of the participants who could detect median antebrachial vein increased in the trial with the system when compared to those in the trial without the system. With respect to the basilic vein and cephalic vein, there are no differences in the number of participants who could detect the vein. However, a participant could detect the cephalic vein with the system, while another participant could not identify the cephalic vein with the system.

	Without system	With system
Median antebrachial vein	1	5
Cephalic vein	4	4
Basilic vein	0	0

Two of the nurses had less than a year of clinical experience, a nurse had 1–3 years of experience, and the remaining two nurses had 3–10 years of experience. A nurse worked for the medical ward while the others worked for the surgical ward.

Without the system, a nurse could detect the median antebrachial vein, four nurses could detect the cephalic vein, and none of the nurses could detect the basilic vein. With the system, five nurses could detect the median antebrachial vein, four nurses could detect the cephalic vein, and none of the nurses could detect the basilic vein. The number of nurses who could detect the median antebrachial vein increased from one to five with the system. The basilic vein was not detected in the anterior surface of the forearm with or without the system. The cephalic vein was detected by three of the four nurses who could detect the vein without the system, but the other nurse could not detect the vein with the system. Additionally, a nurse who could not detect the vein without the system could detect the cephalic vein with the system. The results are shown in **Table 1**.

4. Discussion

In this study, a new US image displaying system to support detecting veins for PIVC was developed and its usefulness was confirmed. The median antebrachial vein was detected with the system by more nurses when compared with the detection without the system. There were two interpretations for this result. First, the US image helped nurses to detect veins that could not be confidently considered as a vein merely by inspection and palpation. Second, the nurses concentrated on the area around the indicated vein in the US image. Conversely, the cephalic vein was detected by four participants in the trial without the system. A participant commented, “I sometimes lost the vein detected once by palpation without the system; however, the system enhanced my confidence on existence of the vein underneath the fingertip.” This comment suggested that the system also aided in increasing confidence in vein selection. The basilic vein could not be detected with or without the system. This is because

the basilic vein runs through almost inner surface of the forearm. The US probe used in the study could offer a narrow image, and it was not possible to scan the vein. This problem was also attributed to the employment of US images acquired through a single scan. An automatic image integration system for US images acquired through multiple scans will solve the narrow range problem by offering panoramic US images of patients’ forearm.

It could be stated that the user interface and operations involving a user’s finger were well-designed. A few participants are familiar with the observations of subcutaneous tissue, particularly in peripheral veins, by US. In the US assessment, the deformation of the vein was often observed in the US image by pressing the skin with a US probe to confirm as to whether a vessel was a vein. In the experiments, an attempt was made to press the skin surface with fingertips that were used as a virtual US probe to observe the deformation of the vein in the US image. This common action for US assessment indicated that the virtual US probe system achieved the same operability as that in the case when a nurse used an actual US probe. However, this system did not reflect the compression by finger. Thinking of the aim of that action, to examine if a vessel is a vein or an artery, displaying veins and arteries in different color will overcome this limitation. Thus, it is desirable to determine an identification system for veins from arteries as well as vessels.

It is expected that the US will be widely used by nurses for vessel assessment. Generally, US is a non-invasive and precise modality that can visualize subcutaneous structures that cannot be visualized by other major modalities, such as magnetic resonance imaging (MRI) or computed tomography (CT), owing to their low-resolution. Additionally, nurses can use US to acquire real-time images of subcutaneous structures with a high-frequency probe at a patient’s bedside. Furthermore, robots assisting precise observation by US were developed [17, 18], and this will lead to the prevalence of US assessment. The combination of the robots and the virtual ultrasonic probe system increases the clinical feasibility of the US-assisted PIVC insertion.

This system is similar to the Real-time Virtual Sonography (RVS) system developed by Hitachi Medical Corporation as this also displays the reconstructed images from pre-scanned images obtained by other modalities, such as CT or MRI, that correspond to the position of US probe. Additionally, RVS is already applied for radio frequency ablation in hepatocellular carcinoma treatment [19]. However, an expensive position sensor, such as the magnetic motion sensor, is required to implement RVS, and pre-scanned CT or MRI images are also required. Thus, it is difficult to apply a RVS to PIVC insertion. In contrast, with respect to the virtual US probe system, US image scanning generates the dataset for virtual image construction, and simple equipment consisting of a head-mounted camera and marker attachment enables nurses to observe a US image without requiring a special sensor. Furthermore, superimposing colored vessels on the US image and displaying the depth and diameter of

veins make the system more useful for the assessment of appropriate veins for PIVC insertion.

Nevertheless, the system involves a limitation. In the proposed system, pre-scanning is performed by a single sweep with the US probe. Therefore, it is not possible to obtain an image of the tissue outside the probe width. The appropriate veins for PIVC are also located on areas other than the anterior surface of the forearm, and thus image reconstruction from multiple scanning will be considered in a future study. Moreover, experiments will be required to examine the effectiveness for PIVC site selection and to evaluate the clinical usability of this system.

5. Conclusions

In this study, a new US image displaying system was realized to support the detection of veins for PIVC insertion. This system displayed virtual cross-sectional US images with vein information, such as vein depth and diameter, on the HMD corresponding to the position and direction of fingertips. The newly developed image-processing algorithm for the head-mounted camera realized a “virtual ultrasonic probe” by robustly detecting the fingertip. The experiment demonstrated that the system could present vein information corresponding to finger movement by US images.

Acknowledgements

The authors are grateful for the feedback by Dr. Ryoko Murayama and technical support provided for US by Mr. Hidenori Tanabe. The HMD AiRScouter WD-200S used in this study was borrowed from Brother Industries, Ltd.

References:

- [1] W. Zingg and D. Pittet, “Peripheral venous catheters: an under-evaluated problem,” *Int. J. Antimicrob. Agents*, Vol.34, No.4, pp. S38-42, 2009.
- [2] C. M. Rickard, J. Webster, M. C. Wallis, N. Marsh, M. R. McGrail, V. French, L. Foster, P. Gallagher, J. R. Gowardman, L. Zhang, A. McClymont, and M. Whitby, “Routine versus clinically indicated replacement of peripheral intravenous catheters: a randomised controlled equivalence trial,” *Lancet*, Vol.380, No.9847, pp. 1066-1074, 2012.
- [3] T. Takahashi, R. Murayama, M. Oe, G. Nakagami, H. Tanabe, K. Yabunaka, R. Arai, C. Komiyama, M. Uchida, and H. Sanada, “Thrombus with subcutaneous edema detected by ultrasonography related to peripheral intravenous catheter failure,” *Congress brochure of The 4th World Congress on Vascular Access*, p. 20, 2016.
- [4] L. C. Hadaway and D. A. Millam, “On the road to successful I.V. starts,” *Nursing (Lond.)*, Vol.35, No.1, pp. S1-14, 2005.
- [5] P. Szmuk, J. Steiner, R. B. Pop, A. Farrow-Gillespie, E. J. Mascha, and D. I. Sessler, “The VeinViewer vascular imaging system worsens first-attempt cannulation rate for experienced nurses in infants and children with anticipated difficult intravenous access,” *Anesth. Analg.*, Vol.116, No.5, pp. 1087-1092, 2013.
- [6] M. J. Kim, J. M. Park, N. Rhee, S. M. Je, S. H. Hong, Y. M. Lee, S. P. Chung, and S. H. Kim, “Efficacy of VeinViewer in pediatric peripheral intravenous access: a randomized controlled trial,” *Eur. J. Pediatr.*, Vol.171, No.7, pp. 1121-1125, 2012.
- [7] R. N. Kaddoum, D. L. Anghelescu, M. E. Parish, B. B. Wright, L. Trujillo, J. Wu, Y. Wu, and L. L. Burgoyne, “A randomized controlled trial comparing the AccuVein AV300 device to standard insertion technique for intravenous cannulation of anesthetized children,” *Paediatr. Anaesth.*, Vol.22, No.9, pp. 884-889, 2012.
- [8] M. D. Witting, S. M. Schenkel, B. J. Lawner, and B. D. Euerle, “Effects of Vein Width and Depth on Ultrasound-Guided Peripheral Intravenous Success Rates,” *J. Emerg. Med.*, Vol.39, No.1, pp. 70-75, 2010.
- [9] J. M. Fields, A. J. Dean, R. W. Todman, A. K. Au, K. L. Anderson, B. S. Ku, J. M. Pines, and N. L. Panebianco, “The effect of vessel depth, diameter, and location on ultrasound-guided peripheral intravenous catheter longevity,” *Am. J. Emerg. Med.*, Vol.30, No.7, pp. 1134-1140, 2012.
- [10] H. Tanabe, T. Takahashi, R. Murayama, K. Yabunaka, M. Oe, Y. Matsui, R. Arai, M. Uchida, C. Komiyama, and H. Sanada, “Using Ultrasonography for Vessel Diameter Assessment to Prevent Infiltration,” *J. Infus. Nurs.*, Vol.39, No.2, pp. 105-111, 2016.
- [11] American Institute of Ultrasound in Medicine, “Use of Ultrasound to Guide Vascular Access Procedures,” *AJUM Pract. Guidel.*, 2012.
- [12] Y. Kobayashi, R. Hamano, H. Watanabe, T. Koike, J. Hong, K. Toyoda, M. Uemura, S. Ieiri, M. Tomikawa, T. Ohdaira, M. Hashizume, and M. G. Fujie, “Preliminary in vivo evaluation of a needle insertion manipulator for central venous catheterization,” *ROBOMECH J.*, Vol.1, No.18, 2014.
- [13] N. Kaneko, M. Sato, T. Takeshima, Y. Sehara, and E. Watanabe, “Ultrasound-guided central venous catheterization using an optical see-through head-mounted display: A pilot study,” *J. Clin. Ultrasound*, Vol.44, No.8, pp. 487-491, 2016.
- [14] N. Hanafusa, T. Torato, and T. Katano, “Future Blood Vessel Puncture Procedure With Use of Head Mount Display,” *Ther. Apher. Dial.*, Vol.20, No.1, pp. 88-89, 2016.
- [15] D. Lee and S. Lee, “Vision-Based Finger Action Recognition by Angle Detection and Contour Analysis,” *ETRI J.*, Vol.33, No.3, pp. 415-422, 2011.
- [16] G. Welch and G. Bishop, “An Introduction to the Kalman Filter,” *Course Notes 8 ACM SIGGRAPH 2001*, 2001.
- [17] Y. Aoki, K. Kaneko, T. Sakai, and K. Masuda, “A study of scanning the ultrasound probe on body surface and construction of visual servo system based on echogram,” *J. Robot. Mechatronics*, Vol.22, No.3, pp. 273-279, 2010.
- [18] K. Ito, S. Sugano, R. Takeuchi, K. Nakamura, and H. Iwata, “Usability and performance of a wearable tele-echography robot for focused assessment of trauma using sonography,” *Med. Eng. Phys.*, Vol.35, No.2, pp. 165-171, 2013.
- [19] Y. Minami, H. Chung, M. Kudo, S. Kitai, S. Takahashi, T. Inoue, K. Ueshima, and H. Shiozaki, “Radiofrequency ablation of hepatocellular carcinoma: value of virtual CT sonography with magnetic navigation,” *AJR. Am. J. Roentgenol.*, Vol.190, No.6, pp. W335-W341, 2008.



Name:

Shuhei Noyori

Affiliation:

Department of Gerontological Nursing/Wound Care Management, Graduate School of Medicine, The University of Tokyo

Address:

7-3-1 Hongo, Bunkyo-ku, Tokyo 113-0033, Japan

Brief Biographical History:

2016 Graduate from The University of Tokyo
2016- Master Course Student, The University of Tokyo

Membership in Academic Societies:

- Japanese society of Wound, Ostomy, and Continence Management
- The Society for Nursing Science and Engineering



Name:
Gojiro Nakagami

Affiliation:
Lecturer, Department of Gerontological Nursing/Wound Care Management, Graduate School of Medicine, The University of Tokyo

Address:

7-3-1 Hongo, Bunkyo-ku, Tokyo 113-0033, Japan

Brief Biographical History:

2009- Research Associate, The University of Tokyo
2010- Lecturer, The University of Tokyo
2013-2014 Visiting Researcher, University of California, Los Angeles

Main Works:

- G. Nakagami, H. Sanada, and J. Sugama, "Development and evaluation of a self-regulating alternating pressure air cushion," Disability and Rehabilitation Assistive Technology, Vol.10, No.2, pp. 165-169, 2011.

Membership in Academic Societies:

- Japanese Society of Pressure Ulcers (JSPU), Councilor
- Japanese Society of Wound, Ostomy, and Continence Management, Councilor
- The Society for Nursing Science and Engineering, Councilor



Name:
Koichi Yabunaka

Affiliation:
Project Assistant Professor, Department of Gerontological Nursing/Wound Care Management, Graduate School of Medicine, The University of Tokyo

Address:

7-3-1 Hongo, Bunkyo-ku, Tokyo 113-0033, Japan

Brief Biographical History:

2005- Department of Ultrasound, Katsuragi Hospital
2014- Department of Gerontological Nursing/Wound Care Management, Graduate School of Medicine, The University of Tokyo

Main Works:

- K. Yabunaka, J. Matsuo, A. Hara, M. Takii, G. Nakagami, T. Gotanda, G. Nishimura, and H. Sanada, "Sonographic visualization of fecal loading in adults: Comparison with computed tomography," The J. of Diagnostic Medical Sonography, Vol.31, No.2, pp. 86-92, 2015.

Membership in Academic Societies:

- Japan Society of Ultrasonics in Medicine
- Japanese Society of Radiological Technology
- The Society for Nursing Science and Engineering



Name:
Hiroshi Noguchi

Affiliation:
Project Lecturer, Department of Life Support Technology (Molten), Graduate school of Medicine, The University of Tokyo

Address:

7-3-1 Hongo, Bunkyo-ku, Tokyo 113-0033, Japan

Brief Biographical History:

2006- Project Research Associate, The University of Tokyo (Researcher, CREST, Japan Science and Technology)
2011- Project Assistant Professor, The University of Tokyo
2015- Project Lecturer, The University of Tokyo

Main Works:

- H. Noguchi, M. Oe, K. Takehara, T. Mori, and H. Sanada, "Reliability and validity of an on-site measurement and visualization system to measure plantar pressure and shear force in footwear for the education of diabetic patients," J. of Japanese Society of Wound, Ostomy, and Continence, Vol.19, No.3, pp. 327-335, 2015.
- nursing engineering, smart home, sensor network, human behavior measurement

Membership in Academic Societies:

- The Robotics Society of Japan (RSJ)
- The Japan Society of Mechanical Engineers (JSME)
- The Institute of Electrical and Electronic Engineers (IEEE) Robotics and Automation Society
- The Society for Nursing Science and Engineering



Name:
Taketoshi Mori

Affiliation:
Project Professor, Department of Life Support Technology (Molten), Graduate school of Medicine, The University of Tokyo

Address:

7-3-1 Hongo, Bunkyo-ku, Tokyo 113-0033, Japan

Brief Biographical History:

1995- Research Associate, The University of Tokyo
1998- Lecturer, The University of Tokyo
2001- Visiting Scientist, Massachusetts Institute of Technology
2002- Associate Professor, Graduate School of Information Science and Technology, The University of Tokyo
2010- Project Associate Professor, Graduate School of Medicine, The University of Tokyo
2015- Project Professor, Graduate School of Medicine, The University of Tokyo

Main Works:

- T. Mori, T. Sato, A. Kuroda, M. Tanaka, M. Shimosaka, T. Sato, H. Sanada, and H. Noguchi, "Outdoor Map Construction Based on Aerial Photography and Electrical Map Using Multi-Plane Laser Range Scan Data," J. of Robotics and Mechatronics, Vol.25, No.1, pp. 5-15, 2013.
- Human-machine systems, behavior understanding, pervasive sensing, sensor networks, motion-based user interface, advanced nursing technology, MIMAMORI engineering.

Membership in Academic Societies:

- The Japan Society of Mechanical Engineers (JSME)
- The Robotics Society of Japan (RSJ)
- The Society of Instrument and Control Engineers (SICE)
- Japanese Society for Medical and Biological Engineering (JSMBE)
- The Institute of Electronics, Information and Communication Engineers (IEICE)
- The Institute of Electrical and Electronic Engineers (IEEE)
- Association for Computing Machinery (ACM)
- The Society for Nursing Science and Engineering

**Name:**

Hiromi Sanada

Affiliation:

Professor, Department of Gerontological Nursing/Wound Care Management, Graduate School of Medicine, The University of Tokyo

Address:

7-3-1 Hongo, Bunkyo-ku, Tokyo 113-0033, Japan

Brief Biographical History:

1979 Graduate from St. Luke's College of Nursing

1981- Research Associate, School of Paramedicine, Kanazawa University

1995- Associate Professor, School of Health Sciences, Faculty of Medicine, Kanazawa University

1998- Professor, School of Health Sciences, Faculty of Medicine, Kanazawa University

2004- Professor, Division of Health Sciences and Nursing, Graduate School of Medicine, The University of Tokyo

Main Works:

- H. Sanada, G. Nakagami, Y. Mizokami, Y. Minami, A. Yamamoto, M. Oe, T. Kaitani, and S. Iizaka, "Evaluating the effect of the new incentive system for high-risk pressure ulcer patients on wound healing and cost-effectiveness: a cohort study," Int. J. Nurs. Stud., Vol.47, No.3, pp. 279-286, 2010.
- Bio-engineering nursing, gerontological nursing, advanced nursing technology, health insurance translational research, wound healing, wound care.

Membership in Academic Societies:

- Japanese Society of Wound, Ostomy, and Continence Management
 - Japanese Society of Pressure Ulcers (JSPU)
 - Japanese Society for Wound Healing (JSWH)
 - Japanese Society of Stoma and Continence Rehabilitation
 - The World Council of Enterostomal Therapists (WCET)
 - Japan Academy of Nursing Science (JANS)
 - The Society for Nursing Science and Engineering
-